RESEARCH PAPER

Synthesis and Characterization of $CoFe_2O_4$ Magnetic Nanoparticles via Combustion Method for Efficient Pb (II) Removal from Wastewater

Pratiksha Jadon[a], Shalini Sharma[b], Sampat G. Deshmukh[c]
[a]Research Scholar, Medicaps University, Indore, 453331, India
[b]Assistant Professor, Medicaps University, Indore, 453331, India
[c]Assistant Professor, SKN Sinhgad College of Engineering, Pandharpur,413304 India
jadounp0101@gmail.com1 shalini.sharma@medicaps.ac.in2
samseeraj2022@gmail.com3

Abstract: Nano-crystalline magnetic particles of $Co_xFe_{(3-x)}O_4$, where x = 0.80–1.01, was prepared by the combustion reaction approach with the use of $Fe(NO_3)_3.9H_2O$, $Co(NO_3)_2.6H2O$, and $CO(NH_2)_2$ as fuels and without templates followed by heat treatment. The process is quite easy and economical because no intermediate steps of decomposition and calcination are necessary. The maximum temperature of combustion ranged from 850 to 1010 1C and took less than 30s in all cases. X-ray diffraction revealed broadened peaks in correspondence with the cubic inverse spinel structure of $CoFe_2O_4$. No presence of additional reflections in the diffraction pattern of prepared material provides pure phases. The crystallite sizes were calculated from the most intensive (311) peak of the diffraction using Scherre's equation. Adsorption processes have been studied in order to provide maximum efficiency of $CoFe_2O_4$. The analyses have shown that % removal of Pb(II) increase with increasing the concentration of cobalt. Specific features of prepared material include easy separation, high adsorption per unit area, economic cost, and possibility of reusing with great efficiency.
Keywords : Adsorption, Combustion, Composition, Equilibrium, Concentration
How to cite this article: Jadona P, Sharma S, Deshmukh SG. Synthesis and Characterization of $CoFe_2O_4$ Magnetic Nanoparticles via Combustion Method for Efficient Pb (II) Removal from Wastewater. Int J Drug Deliv Technol. 2026;16(70s): 1551-1560. DOI: 10.25258/ijddt.16.70s.167

1. Introduction

The accelerated growth of industrial activities has caused the discharge of significant volumes of sewage that remain untreated or only partially treated. [1] This sewage contains chemical contaminants and toxic metals, which are released to the surroundings either directly or through indirect pathways. The environmental discharge of these metals has been significantly influenced by human activities, including industrial manufacturing, mining, and the application of metals in various products.
In ecological systems, metals like copper, arsenate, lead, cadmium, and mercurial compounds, exhibit extremely high levels of toxicity, radioactivity, and radio- toxicity [2]. As a result, this waste enters lakes, oceans, and rivers, contributing to water pollution and posing serious risks to the survival of living organisms [3–5].
Lead Pb(II) was derived from various industries such as battery manufacturing and metal plating. Besides, Pb(II) can accumulate in human bodies and lead to many serious diseases, such as anemia, sterility, hypertension, nephritic syndrome and hepatitis [6].
Therefore, it is necessary to remove Pb(II) for providing safety living environment for human. To solve this issue, several methods have been developed to remove Pb(II) from wastewater, varying in effectiveness, economic cost and environment impact, such as chemical precipitation, ion exchange, membrane separation and adsorption technology [7-8].

Among all the method proposed, the adsorption of Pb(II) onto a substrate can be high efficiency, easy operation, low-cost and environmental friendless [9-10]. Up to now, various adsorbents have been developed for the removal of Pb(II). However, most of adsorbent materials are not the ideal choices for their difficulty of separation from solution in application, resulting in the secondary pollution.

The unique properties of magnetic nanoparticles (MNPs) have recently garnered significant attention in environmental science [11]. The modification of these nanoparticles can be achieved by using external magnetic fields. In addition, they are com- posed of elements such as oxygen, cobalt, nickel, and iron and have a very small particle size [12-13]. The surface functionalization of

nanomaterial's involves adding a functional group selectively to the surface without affecting the main characteristics. A surface functionalized material has new surface chemical properties that differ from its original properties, such as reactivity, solubility, melting point, stability, and electronic structure [14]. The coating also results in a homogeneous size distribution, well-defined shape distribution, and controllable stability in water [15].

The toxic elements are used in numerous industrial processes, leaving harmful impacts on human health. Heavy metals are well-thought-out hazard for living creatures as they are poisonous and non-biodegradable leading to the rising of concentration of a chemical in living organisms and can be accumulated through the food chain. Compounds are accumulated in living organisms by uptake from environment and storage at a higher rate than that of metabolism or excretion [16-17]. Heavy metals may cause liver damage, renal failure, cardiovascular diseases, and even death [18]. Several techniques have been investigated for heavy metals and dye uptake from wastewater such as photo catalytic, chemical oxidation, adsorption, biodegradation, and electrochemistry.

It underscores the need for innovative methods to remove heavy ions from industrial effluents. Various materials have been utilized to extract harmful metal ions, including bio- mimetic compounds, ion exchange resins, activated carbon, hydrogels; Nano sized materials, and biopolymers [19–22].

In terms of cost-effectiveness, MNP adsorption is the most effective way to remove potentially toxic elements.

Adsorption is the process that is utilized for the removal of heavy metals from wastewater. Many researches have been conducted to remove heavy metals using various materials. Numerous adsorbents have been used to eliminate different types of heavy metal ions from wastewater specifically those that are hurtful to mankind. One of the most common adsorbents is Nano ferrite particles [23].

Adsorbent properties, including specific surface area and particle sizes, are the essential factors that affect the adsorption efficiency. Therefore, synthesizing and developing an effective adsorbent is significant in the water treatment applications [24].

The magnetic nanoparticles due to several advantages such as the feasibility of preparation, easy separation (by an external magnetic field), high surface areas, and high chemical and mechanical stability attract increasing attention as potential adsorbents for heavy metal removal from aqueous solutions [25-28]. In the past decades, various magnetic materials, including a type of ferrites, $M^{II}Fe_2O_4$ (M = Co, Zn, Mg, Cu, etc.), have been widely used in different technological applications [29]. Among the possible ferrite materials, $CoFe_2O_4$ is an interesting candidate for adsorption applications due to moderate saturation magnetization, exceptional chemical stability, and adequate mechanical hardness [30].

Cobalt ferrite is one of the more malleable; therefore, it is a crucial spinel compound; it has an inverse spinel structure. It can be used as an electro catalyst apart from its electric and magnetic applications, due to its conducting nature. Cobalt ferrite is preferred due to relatively low magnetic loss, high saturation magnetization, temperature stability, and biodegradability.

$CoFe_2O_4$ MNPs distinguish among these MNPs due to their distinctive chemical and physical characteristics, including coercivity, high magnetism, and mechanical toughness [31-33]

Uncoated magnetite nanoparticles, however, have poor adsorption characteristics and are more susceptible to oxidation and agglomeration.

In recent years, several synthetic methods to prepare highly crystalline and uniformly sized magnetic nanoparticles of cobalt ferrite have been report. However, most of these methods cannot be applied to a large- scale and economic production because they require expensive and often toxic reagents, complicated synthetic steps, high reaction temperature and long reaction time.

Among the current methods for synthesis of cobalt ferrite the combustion reaction stands out as an alternative and highly promising method for the synthesis of these ferrite. This method is quite simple, fast and inexpensive since it does not involve intermediate decomposition and/or calcining steps. Furthermore, it is easy to control the stoichiometry and crystallite size which have important influence on the magnetic properties of the ferrite. The basis of the combustion synthesis technique comes from the thermochemical concepts used in propellant chemistry and explosives. This method exploits an exothermic, usually very rapid and self- sustaining chemical reaction between the desired metal salts and a suitable organic fuel, usually urea. A key feature of this method is that the heat required to sustain the chemical reaction is provided by the reaction itself and not by an external source. The resulting product is a crystalline dry agglomerated into highly fluffy foam with high chemical homogeneity and purity.

The purpose of this work is to prepare and characterize nanoparticles of cobalt ferrite, $Co_xFe_{(3-x)}O_4$, with x ranging from 0.80 to 1.08 by combustion reaction method without subsequent calcination and as well as to investigate their magnetic properties.

2. Experimental procedure

2.1 Chemicals

The nanoparticles of cobalt ferrite were synthesized by combustion reaction using analytical grade iron nitrate $Fe(NO_3)_3 \cdot 9H_2O$, cobalt nitrate $Co(NO_3)_2 \cdot 6H_2O$, and urea $CO(NH_2)_2$ as fuel. Manipulations and reactions were carried out in air without the protection of nitrogen or inert gas.

2.2 Synthesis

The stoichiometric composition of each mixture was calculated based on the total oxidizing and reducing valences of the oxidizer and fuel which serve as numerical coefficients for stoichiometric balance so that the equivalent ratio is unity and the release energy is maximum for each reaction. According to the thermochemical concepts from propellant chemistry, the elements H, C, Co and Fe are considered as reducing elements, element oxygen is considered as an oxidizing element, and the valency of element nitrogen is considered to be zero [34]. Thus the total valences in $Fe(NO_3)_3.9H_2O$ adding up to —15 and $Co(NO_3)_2.6H_2O$ add up to —10 should be balanced by the total valences in the fuel, which add up to +6. Hence the stoichiometric composition of the redox mixture in order to release the maximum energy for the reaction, require that $-40+6n = 0$ or $n = 6.67$ mole of urea. For instance, to prepare $CoFe_2O_4$, the reactants should be combined in a molar proportion of 1:2:6.67 of $Co(NO_3)_2.6H_2O$, $Fe(NO_3)_3.9H_2O$ and urea $CO(NH_2)_2$, shown in Fig 1 respectively. Therefore, based on that, the stoichiometric molar proportion were calculated for batches of $Co_xFe_{(3-x)}O_4$ with $x = 0.80$, 0.89, and 1.01.

The reactants were hand mixed in a wide mouth vitreous silica basin of 300 cm^3 and heated up to around 400 1C on a hot blanket inside a fume cupboard, under ventilation. With a rise in temperature, melting occurred and a dark liquid was produced, which boiled and thickened. Soon after the thickened liquid began frothing, ignition took place, leading to rapid increase in temperature, appearance of a central point of incandescence that propagated in swift ripples to walls of the basin, and evolution of a large quantity of gases mention in Fig 2. The reaction was quite fast and produced a dry, very fragile foam, which transformed into powder at slightest touch.

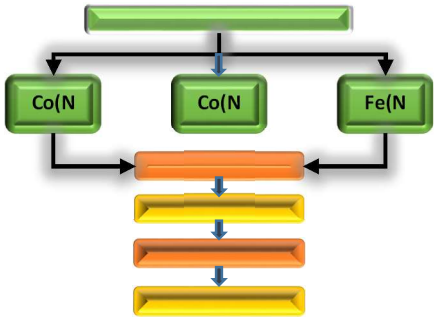

Fig 1. Synthesis of $CoFe_2O_4$ Nanoparticles

Fig 2. Flame Produced during Combustion Reaction

2.3 CHARACTERIZATION

The as-prepared powder was characterized by X-ray diffraction (XRD) using a Shimadzu diffractometer (model 6000) with CuKa radiation (l ¼ 1.5418A˚) in a wide range of Bragg angles ($15^o < 20^o < 80^o$) with a scanning rate of 21 min^{-1} at room temperature. The

average crystallite size were calculated from X-ray line broadening using (3 1 1) peaks and Scherre's equation.

$$D = K\lambda / (\beta \cos \theta) \quad (1)$$

The full width at half maximum (β) of a peak in a substance's X-ray diffraction (XRD) pattern, wherein K is an integer, λ is the X-ray and θ is the Bragg angle, is used to calculate the mean size of the crystals (D).

2.4 Batch Experiment of Heavy Metal Removal

To study the optimum pH values of heavy metal (Pb^{2+}) removal, the experiments were carried out in a series of 250-mL flasks containing 0.1 g/L of $CoFe_2O_4$ nanomaterial powder in 2 ppm of metals nitrate. Metal ions adjusted at different pH values from 2 to 8. The initial pH of the solution was adjusted with either HCl or NaOH. The investigated solutions were dispersed well using electric shaker at 250 rpm for 60 min at room temperature. The supernatant solutions were then collected and filtered through a 0.2-μm syringe filter. The optimum contact time was elucidated by repeating the above step with adjusting the pH value at its optimum value, and the atomic absorption was measured after different contact times. The nanomaterial removal efficiency and equilibrium adsorption capacity of metal ions were calculated as follows

$$\text{Removal (adsorption) efficiency} = \frac{C_0 - C_e}{C_0} \times 100\ \% \quad (2)$$

Where, C_0 and C_e are the initial and equilibrium (final) concentrations (mg/L) of metal ion solution, respectively,

3. Result & Discussion

3.1 Chemical Reactions

The synthesis of Cobalt ferrite nanoparticles was carried out by the homogeneous precipitation method using Cobalt(II) nitrate hexahydrate and Iron(III) nitrate Nona hydrate as metal precursors, while Urea was employed as a precipitating agent. In this method, the aqueous solution containing cobalt and iron nitrates in a stoichiometric molar ratio of 1:2 was heated at 80–90 °C under constant stirring. Upon heating, urea undergoes slow hydrolysis to generate ammonia and carbon dioxide. The released ammonia further reacts with water to produce hydroxide ions, leading to a gradual increase in the pH of the solution.

$$CO(NH_2)_2 + H_2O \rightarrow 2NH_3 + CO_2 \quad (3)$$

Ammonia further reacts:

$$NH_3 + H_2O \rightarrow NH^{4+} + OH^- \quad (4)$$

From the above reactions it has been understood that the decomposition of urea is highly exothermic, aiding the decomposition of nitrates salts into desired products at a faster rate with low external-energy consumption. Urea is considered to be more suitable organic fuel than tetraformal triazine ($C_4H_{16}N_6O_2$), maleic hydrazide ($C_4H_4N_2O_2$) and carbohydrazide ($CO(N_2H_3)_2$) because it is readily available commercially, cheap, and generates the highest temperature during combustion.

These hydroxide ions facilitate the uniform precipitation of cobalt and iron ions in the form of their respective hydroxides according to the reactions:

$$Co^{2+} + 2OH^- \rightarrow Co(OH)_2 \quad (5)$$

The resulting mixed hydroxide precursor, $Co(OH)_2 + 2Fe(OH)_3$, was filtered, washed, and dried, followed by calcination at elevated temperature to obtain crystalline cobalt ferrite. During calcination, the hydroxide precursor undergoes dehydration and solid-state reaction to form the spinel phase as represented below:

$$Co(OH)_2 + 2Fe(OH)_3 \rightarrow CoFe_2O_4 + 4H_2O \quad (6)$$

The overall reaction can be summarized as:

$$Co(NO_3)_2 \cdot 6H_2O + 2Fe(NO_3)_3 \cdot 9H_2O + 8CO(NH_2)_2 \rightarrow CoFe_2O_4 + 8NH_4NO_3 + 4CO_2 + 20H_2O \quad (7)$$

This controlled homogeneous precipitation approach ensures uniform nucleation, better compositional homogeneity, and formation of phase-pure spinel $CoFe_2O_4$ nanoparticles suitable for magnetic and adsorption applications.

3.2 XRD Analysis

X-ray diffraction (XRD) is carried out for the pure $CoFe_2O_4$ nanoparticles to scrutinize the structure of the synthesized samples. In Fig. 3 the XRD patterns ratify the formation of the cubic spinel structure for the prepared samples in a single phase.

The XRD pattern of the synthesized magnetite $CoFe_2O_4$ nanoparticles indicates the presence of the characteristic peaks of (220), (311), (400), (511), and (440), which were observed at the diffraction angles of 2Θ = 30.23, 35.69, 43.26, 57.29, and 62.83, respectively. These peaks are the main characteristic peaks of $CoFe_2O_4$, which confirm that the resultant nanoparticles are pure $CoFe_2O_4$. As can be observed, the position and intensities of nearly all of the peaks are well matched to those of the other experimental results and the standard PDF cards for $CoFe_2O_4$ nanoparticles (JCPDS: 00-022-1086).

Table:1 Some physical characteristics of $CoFe_2O_4$ sample prepared by combustion reaction

Sample	Composition%	Crystalline size (nm)	Crystallinity(%)
(S1) Pure Fe_3O_4	0	38.45 nm	64.3%
(S2) $CoFe_2O_4$	0.80	4.46 nm	65.0%
(S3) $CoFe_2O_4$	0.89	3.61 nm	65.4%
(S4) $CoFe_2O_4$	1.01	3.57 nm	76.3%

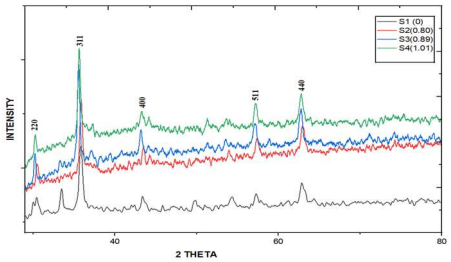

Fig 3. XRD Patterns of $CoFe_2O_4$ (JCPDS: 00-022-1086)

3.3 Adsorption tests

3.3.1 Effect of $CoFe_2O_4$ Composition on Lead Removal

The adsorption behavior of lead (Pb^{2+}) ions onto $CoFe_2O_4$ nanoparticles was investigated by varying the composition parameter (x) from 0.00 to 1.01. The initial lead concentration (C_0) in the untreated water sample was 3.95 mg L^{-1}. Following treatment with $CoFe_2O_4$ nanoparticles, the residual lead concentration decreased significantly, indicating successful adsorption of Pb^{2+} ions from the aqueous medium.

The equilibrium concentration (C_e) decreased from 3.95 mg L^{-1} in the untreated sample (x = 0.00) to 3.42, 2.32, and 2.28 mg L^{-1} for x values of 0.80, 0.89, and 1.01, respectively. In Fig.4 the continuous decrease in equilibrium concentration with increasing x demonstrates that the adsorption efficiency of the material improved as the $CoFe_2O_4$ composition increased.

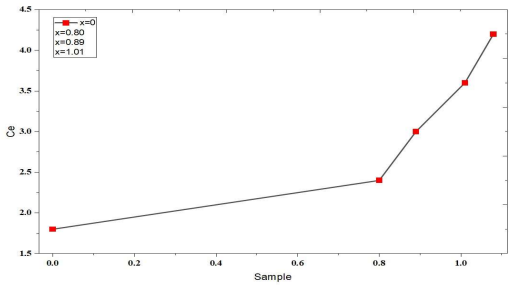

Fig 4. Effect of sample composition (X) on the equilibrium concentration (C_e) of fluoride after adsorption. The equilibrium concentration decreased from **3.95 mg L^{-1}** to **2.28 mg L^{-1}** with increasing sample composition, indicating enhanced adsorption performance.

The reduction in lead concentration can be attributed to the presence of a larger number of accessible adsorption sites and enhanced surface reactivity of the $CoFe_2O_4$ nanoparticles. Metal oxide nanoparticles are known to possess high specific surface area and abundant surface hydroxyl groups, which facilitate the binding of heavy metal ions through electrostatic attraction, surface complexation, and ion-exchange processes.

3.3.2 Adsorption Capacity Analysis

The adsorption capacity (Q_e) represents the amount of lead adsorbed per unit mass of adsorbent and was calculated using the equation:

$$Qe = \frac{(C_0 - Ce)\,V}{m}$$

where:

- (Qe) = adsorption capacity (mg g^{-1})
- (C_0) = initial lead concentration (mg L^{-1})
- (Ce) = equilibrium lead concentration (mg L^{-1})
- (V) = volume of solution (0.25 L)
- (m) = mass of adsorbent (0.025 g)

The calculated adsorption capacities were 5.30, 16.30, and 16.70 mg g^{-1} for x values of 0.80, 0.89, and 1.01, respectively.

The increase in adsorption capacity with increasing x value suggests that the modification of $CoFe_2O_4$ composition enhanced the affinity of the adsorbent toward Pb^{2+} ions shows in Fig.5. A higher adsorption capacity indicates that more lead ions were retained on the adsorbent surface, demonstrating the effectiveness of $CoFe_2O_4$ nanoparticles as an adsorbent material.

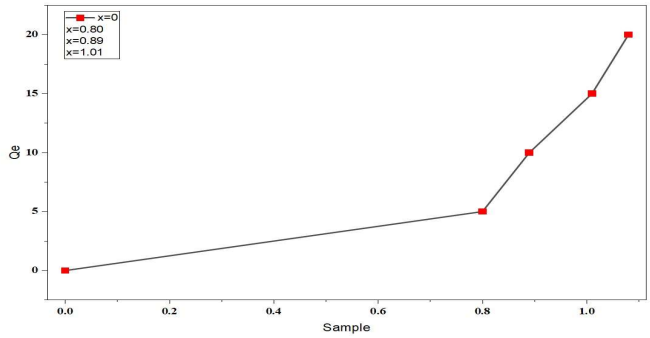

Fig 5. Effect of sample composition (X) on the equilibrium adsorption capacity (q_e) of the adsorbent for lead removal.

The maximum adsorption capacity of 16.70 mg g^{-1} obtained at x = 1.01 indicates that the synthesized material possesses a substantial number of active adsorption sites capable of interacting with dissolved lead ions. The relatively small difference between the adsorption capacities at x = 0.89 and x = 1.01 suggests that the adsorption process approaches saturation at higher composition values.

3.3.3 Removal Efficiency of Lead Ions

The percentage removal efficiency was determined using the following equation:

$$\text{Removal (adsorption) efficiency} = \frac{C_0 - Ce}{C_0} \times 100\ \%$$

The calculated removal efficiencies were 13.42%, 41.27%, and 42.28% for x values of 0.80, 0.89, and 1.01, respectively.

The results reveal a strong dependence of lead removal efficiency on the $CoFe_2O_4$ composition. A sharp increase in removal efficiency was observed between x = 0.80 and x = 0.89, indicating that compositional modification significantly improved the adsorption performance. Fig.6 shows the highest removal efficiency of 42.28% was achieved at x = 1.01, corresponding to the lowest equilibrium lead concentration (2.28 mg L^{-1}).

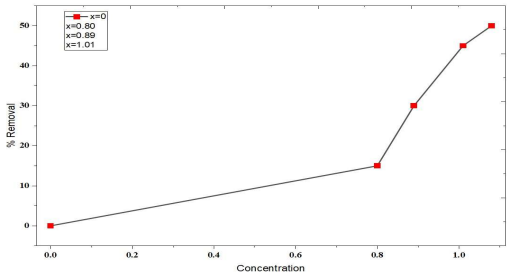

Fig 6. Effect of sample composition (X) on lead removal efficiency. The removal efficiency increased with increasing X value

The enhanced removal efficiency may be attributed to improved surface characteristics, increased surface charge density, and greater availability of active adsorption sites. These factors facilitate stronger interactions between Pb^{2+} ions and the adsorbent surface, resulting in more effective removal of lead from the aqueous phase.

3.3.4 Adsorption Mechanism

The adsorption of Pb^{2+} ions onto $CoFe_2O_4$ nanoparticles is likely governed by multiple physicochemical interactions. The surface of $CoFe_2O_4$ contains hydroxyl groups and oxygen-containing functional sites capable of interacting with dissolved lead ions. During adsorption, Pb^{2+} ions migrate from the bulk solution to the adsorbent surface, where they become attached through electrostatic attraction and surface complexation reactions.

In addition, the magnetic spinel structure of $CoFe_2O_4$ provides structural stability and a large number of adsorption sites. The porous nature and nanoscale dimensions of the particles contribute to enhanced diffusion of metal ions and improved adsorption kinetics. As the composition parameter x increases, the density of available adsorption sites may increase, resulting in greater adsorption capacity and higher removal efficiency.

Table:2 Adsorption parameters and removal efficiency of Pb^{2+} ions using $CoFe_2O_4$ nanoparticles.

Sample (x)	**Initial Concentration,C_0 (mg L^{-1})**	**Equilibrium Concentration,C_e(mg L^{-1})**	**Adsorption Capacity,q_e (mg g^{-1})**	**Removal Efficiency (%)**
X=0	3.95	3.95	0.00	0.00
X=0.80	3.95	3.42	5.30	13.42
X=0.89	3.95	2.32	16.30	41.27
X=1.01	3.95	2.28	16.70	42.28

3.3.5 Environmental Significance

Lead is one of the most toxic heavy metals commonly found in industrial wastewater, mining effluents, and contaminated groundwater. Exposure to lead can cause severe health effects, including neurological, renal, and cardiovascular disorders. Therefore, the development of efficient and economical adsorbents for lead removal is of considerable environmental importance.

The present results demonstrate that $CoFe_2O_4$ nanoparticles can effectively reduce lead concentrations in contaminated water. The decrease in equilibrium concentration, increase in adsorption capacity, and improvement in removal efficiency collectively indicate that $CoFe_2O_4$ is a promising adsorbent for heavy-metal remediation. Furthermore, the magnetic nature of $CoFe_2O_4$ offers an additional advantage, as the adsorbent can be easily separated from treated water using an external magnetic field, making it suitable for practical wastewater treatment applications.

Overall, the findings confirm that increasing the $CoFe_2O_4$ composition enhances the adsorption performance toward Pb^{2+} ions, with x = 1.01 exhibiting the highest adsorption capacity and removal efficiency among the investigated samples

4. Conclusion:

Rapid industrialization has resulted in untreated sewage containing toxic metals like Pb(II), which possess severe risks to the ecosystem and human health. To address this issue Nano crystalline magnetic particles of $CoFe_2O_4$ have been synthesized by combustion reaction method using iron nitrate $Fe(NO_3)_3 \cdot 9H_2O$, cobalt nitrate $Co(NO_3)_2 \cdot 6H_2O$, and urea $CO(NH_2)_2$ as fuel. XRD patterns of all systems showed broad peaks consistent with cubic inverse spinel structure of $CoFe_2O_4$. The absence of extra reflections in the diffraction patterns of as-prepared materials ensures the phase purity. The combustion reaction method produces powders, without intermediate

decomposition or further calcining steps, with magnetic properties, comparable to those of similar powders synthesized by different methods. The synthesized nanoparticles have shown promising results, with high adsorption capacities and good reusability. The adsorption process were studied and optimized in order to achieve the maximum possible adsorption efficiency of the $CoFe_2O_4$ The analyses reveal that % removal of Pb(II) were increased as concentration increased of cobalt. The specific advantages of the prepared samples are ease of separation, high adsorption per unit area, low cost as well as recycled with remarkable efficiency.

References:

1.B. Alqassem, F. Banat, G. Palmisano, and M. Abu Haija,"Emerging Trends of Ferrite-Based Nanomaterials as Photocatalysts for Environmental Remediation: A Review and Synthetic Perspective," *Sustainable Materials and Technologies* 40 (2024): e00961, https://doi.org/10.1016/j.susmat.2024.e00961.

2. L. Fang, T. Huang, H. Lu, et al., "Biochar-Based Materials in Environmental Pollutant Elimination, H_2 Production and CO_2 Capture Applications," *Biochar* 5, no. 1 (2023): 42, https://doi.org/10.1007/s42773-023-00237-7.

3. Y. Huang, Y. Wu, W. Ding, et al., "Anion-Synergistic Ad- sorption Enhances the Selective Removal of Silver Ions From Complex Wastewater by Chitosan-Coated Magnetic Silica Core-Shell Nanoparticles," *Journal of Cleaner Production* 339 (2022): 130777, https://doi.org/10.1016/j.jclepro.2022.130777.

4 A. Choudhry, A. Sharma, T. A. Khan, and S. A. Chaudhry, "Flax Seeds Based Magnetic Hybrid Nanocomposite: An Advance and Sustainable Material for Water Cleansing," *Journal of Water Process Engineering* 42 (2021): 102150, https://doi.org/10.1016/j.jwpe.2021.102150.

5. P. L. Hariani, M. Said, S. Salni, N. Aprianti, and Y. A. L. R. Naibaho, "High Efficient Photocatalytic Degra- dation of Methyl Orange Dye in an Aqueous Solution by $CoFe_2O_4$-SiO_2-TiO_2 Magnetic Catalyst," *Journal of Ecological Engineering* 23, no. 1 (2022): 118–128, https://doi.org/ 10.12911/22998993/143908.

6. Hu, L.H., Yang, Z.P., Cui, L.M., Li, Y., Ngo, H.H., Wang, Y.G., Du, B. 2016.Fabrication of hyperbranched polyamine functionalized graphene for high-efficiency removal of Pb(II) and methylene blue. Chem. Eng. J. 287, 545-556.

7. Fu, F.L., Xie, L.P., Tang, B., Wang, Q., Jiang, S.X. 2012. Application of a novel strategy Advanced Fenton-chemical precipitation to the treatment of strong stability chelated heavy metal containing wastewater. Chem. Eng. J. 189, 283-287.

8. Kanagaraj, P., Nagendran, A., Rana, D., Matsuura, T., Neelakandana, S., Karthikkumar, T., Muthumeenal, A. 2015. Influence of N-phthaloyl chitosan on poly (ether imide) ultrafiltration membranes and its application in biomolecules and toxic heavy metal ion separation and their antifouling properties. Appl. Surf. Sci. 329, 165-173.

9. Guo, S.Z.J., Dan, Z.G.; Duan, N.; Zhang, J. ; Chen, G.Y. ; Gao, W.B. 2017. Synthesis of magnetic bioadsorbent for adsorption of Zn(II), Cd(II) and Pb(II) ions from aqueous solution. Chem. Eng. Res. Des. 126, 217-231.

10. Wu, S.P.W., Yuan, H.K., Zhang, L.J., Mao, S.M., Liu, X.J., Alharbi, N.S., Rohani, S., Lu, J. 2018. Fabrication of xanthate-modified chitosan/poly(N-isopropylacrylamide) composite hydrogel for the selective adsorption of Cu(II), Pb(II) and Ni(II) metal ions. Chem. Eng. Res. Des. 139, 197-210.

11. F. Talebzadeh, R. Zandipak, and S. Sobhanardakani, "CeO_2 Nanoparticles Supported on $CuFe_2O_4$ Nanofibers as Novel Adsorbent for Removal of Pb(II), Ni(II), and V(V) Ions From Petrochemical Wastewater," *Desalination and Water Treat- ment* 57, no. 58 (2016): 28363–28377, https://doi.org/10.1080/19443994.2016.1188733.

12. K. Maaz, A. Mumtaz, S. Hasanain, and A. Ceylan, "Synthesis and Magnetic Properties of Cobalt Ferrite ($CoFe_2O_4$) Nanoparticles Prepared by Wet Chemical Route," *Journal of Magnetism and Magnetic Materials* 308, no. 2 (2007): 289–295, https://doi.org/10.1016/j.jmmm.2006.06.003.

13. L. H. Reddy, J. L. Arias, J. Nicolas, and P. Couvreur, "Magnetic Nanoparticles: Design and Characterization, Toxicity and Biocompatibility, Pharmaceutical and Biomedical Applica- tions," *Chemical Reviews* 112, no. 11 (2012): 5818–5878, https://doi.org/10.1021/cr300068p.

14. M. O. Ojemaye, O. O. Okoh, and A. I. Okoh, "Surface Modified Magnetic Nanoparticles as

Efficient Adsorbents for Heavy Metal Removal from Wastewater: Progress and Prospects," *Materials Express* 7, no. 6 (2017): 439–456, https:// doi.org/10.1166/mex.2017.1401.]

15. Y. Zhu, S. Murali, W. Cai, et al., "Graphene and Graphene Oxide: Synthesis, Properties, and Applications," *Advanced Materials* 22, no. 35 (2010): 3906–3924, https://doi.org/ 10.1002/adma.201001068.

16. H.S. Jahin, A.S. Abuzaid, A.D. Abdellatif, Environ. Technol. Innov. **17**, 100532 (2020)

17. K. Bhuvaneswari, V. Vaitheeswari, G. Palanisamy, T. Maiyalagan, T. Pazhanivel, Mater. Sci. Semicond. Process. **106**, 104760 (2020)

18 N. Ahmad, S. Sultana, S. Sabir, M.Z. Khan, J. Photochem. Pho- tobiol. A **386**, 112129 (2020)

19. M. Arif, T. Muhmood, M. Zhang, et al., "Highly Visible-Light Active, Eco-Friendly Artificial Enzyme and 3D $Bi_4Ti_3O_{12}$ Biomimetic Nanocomposite for Efficient Photocatalytic Tet- racycline Hydrochloride Degradation and Cr(VI) Reduction," *Chemical Engineering Journal* 434 (2022): 134491, https:// doi.org/10.1016/j.cej.2021.134491.

20. B. Fouda-Mbanga, E. Prabakaran, and K. Pillay, "Carbohy- drate Biopolymers, Lignin Based Adsorbents for Removal of Potentially Toxic Elements (Cd^{2+}, Pb^{2+}, Zn^{2+}) From Waste- water, Regeneration and Reuse for Spent Adsorbents In- cluding Latent Fingerprint Detection: A Review," *Biotechnology Reports* 30 (2021): e00609, https://doi.org/ 10.1016/j.btre.2021.e00609.

21. M. Sultana, M. H. Rownok, M. Sabrin, M. H. Rahaman, and S. M. N. Alam, "A Review on Experimental Chemically Modified Activated Carbon to Enhance Dye and Heavy Metals Adsorption," *Cleaner Engineering and Technology* 6 (2022): 100382, https://doi.org/10.1016/j.clet.2021.100382.

22. V. Dhiman and N. Kondal, "ZnO Nanoadsorbents: A Potent Material for Removal of Heavy Metal Ions From Wastewater," *Colloid and Interface Science Communications* 41 (2021): 100380, https://doi.org/10.1016/j.colcom.2021.100380.

23. D.H.K. Reddy, Y.S. Yun, Coord. Chem. Rev. **315**, 90 (2016

24. Zhang Y, Yan L, Xu W, Guo X, Cui L, Gao L et al (2014) Adsorption of Pb(II) and Hg(II) from aqueous solution using magnetic $CoFe_2O_4$-reduced graphene oxide. J Mol Liq 191:177–182

25. Fan FL, Qin Z, Bai J, Rong WD, Fan FY, Tian W et al (2012) Rapid removal of uranium from aqueous solutions using mag- netic Fe_3O_4@SiO_2 composite particles. J Environ Radioact 106:40–46

26. Xin X, Wei Q, Yang J, Yan L, Feng R, Chen G et al (2012) Highly efficient removal of heavy metal ions by amine-func- tionalized mesoporous Fe_3O_4 nanoparticles. Chem Eng J 184:132–140

27. Zhao L, Zhang H, Xing Y, Song S, Yu S, Shi W et al (2008) Studies on the magnetism of cobalt ferrite nanocrystals synthe- sized by hydrothermal method. J Solid State Chem 181(2):245–252

28. Tan L, Liu Q, Jing X, Liu J, Song D, Hu S et al (2015) Removal of uranium (VI) ions from aqueous solution by magnetic cobalt ferrite/multiwalled carbon nanotubes composites. Chem Eng J 273:307–315

29. Baruwati B, Nadagouda MN, Varma RS (2008) Bulk synthesis of monodisperse ferrite nanoparticles at water–organic interfaces under conventional and microwave hydrothermal treatment and their surface functionalization. J Phys Chem C 112(47):18399–18404

30. Liu XM, Fu SY, Zhu LP (2007) High-yield synthesis and char- acterization of monodisperse sub-microsized $CoFe_2O_4$ octahedra. J Solid State Chem 180(2):461–466

31. X. Wang, Z. Zhang, Y. Zhao, et al., "A Mild and Facile Synthesis of Amino Functionalized $CoFe_2O_4$@SiO_2 for Hg (II) Removal," *Nanomaterials* 8, no. 9 (2018): 673, https://doi.org/ 10.3390/nano8090673.

32. A. Benettayeb, F. Z. Seihoub, P. Pal, et al., "Chitosan Nanoparticles as Potential Nano-Sorbent for Removal of Toxic Environmental Pollutants," *Nanomaterials* 13, no. 3 (2023): 447, https://doi.org/10.3390/nano13030447.

33. H. Zhu, Y. Shen, Q. Wang, et al., "Highly Promoted Removal of Hg (II) With Magnetic $CoFe_2O_4$@SiO_2 Core–Shell Nanoparticles Modified by Thiol Groups," *RSC Advances* 7, no. 62 (2017): 39204–39215, https://doi.org/10.1039/ c7ra06163c.

34. S.R. Jain, K.C. Adiga, V.R. Pai Vernecker, Combust. Flame 40 (1981) 71